Nonadiabatic sliding model for rearrangement collisions

D. H. Jakubassa-Amundsen

Physik-Department, Technische Universität München, 8046 Garching, Germany

(Received 15 February 1985; revised manuscript received 8 April 1985)

Using Demkov's variational principle, the probability for electronic excitation is evaluated with the help of optimized basis states, which allow for a continuous transition from an atomic to a molecular description. The inclusion of cosliding translational factors provides an extension to transfer processes. Calculations are performed for radiative electron capture (REC) of a target K electron in the collision systems $^{16}O \rightarrow {}^{12}C$ and $^{32}S \rightarrow {}^{20}Ne$. It is shown that even for fast collisions, an atomic description is only applicable in the REC peak region, while molecular effects have to be included in the tails.

I. INTRODUCTION

For years there has been an unexplained discrepancy between theory and experiment concerning the spectra of photons which are emitted in energetic ion-atom collisions. A prominent peak near $v^2/2$, where v is the collision velocity, has been readily identified as arising from the radiative capture of target electrons by the projectile,[1,2] and the peak intensity as well as the shape of the spectrum in the peak region could satisfactorily be explained within the impulse approximation.[2-4] However, for frequencies well above the peak, the experimental intensity was found to be much higher than predicted by the impulse approximation.[2,4,5] Background effects such as secondary-electron bremsstrahlung or radiative ionization could only partly account for the missing intensity.[4,6]

It has been argued by Betz that, as in slow collisions, the high-energy photons may result from molecular-orbital (MO) radiation[7-9] because a large momentum transfer is required. For slow collisions, two different models are used for the description of the radiative-electron-capture (REC) peak and the tails, respectively,[7] the atomic one for the peak and the molecular one for the tails. As peak and tails originate from the same radiative process,[3] it should be more appropriate to use only one model for both. This can readily be done by means of a variational calculation where atomic *and* molecular properties are incorporated into the wave functions, and which in addition is not restricted to small collision velocities.

The model described below follows the ideas of Stevenson:[10] The estimate of a physical observable within a given order of perturbation theory can be improved by introducing auxiliary parameters into the theory, which are calculated from the principle of "minimal sensitivity" by minimizing the dependence of the observable on these parameters. For one interested in the transition probability, as in the present case, Demkov[11] has provided a profound basis for these ideas through a variational principle: The transition amplitude (and thus the probability) for an arbitrary inelastic process is stationary with respect to variations of the wave functions appearing in the transition amplitude. When auxiliary parameters are contained in the wave functions, they are thus determined from the extremum of the transition probability.

In the nonadiabatic sliding model,[12] one parameter is introduced into the Hamiltonian which determines the portion of the perturbing projectile field that is not incorporated into the wave functions. By varying the portion from one to zero, the wave functions consequently change from atomic to molecular ones. This property led to a successful application of the sliding model to the calculation of δ-electron spectra in medium-energy collisions.[13]

The model presented in this work is an extension of the sliding model to transfer reactions. In Sec. II it is formulated for radiative electron capture. The photon distribution for REC is evaluated within a simplified model description in Sec. III. Numerical results for REC from ^{12}C by ^{16}O impact, and from ^{20}Ne by ^{32}S impact are given in Sec. IV. A short conclusion follows (Sec. V). Atomic units (a.u.) ($\hbar = m = e = 1$) are used unless otherwise indicated.

II. THE SLIDING-CENTER MODEL FOR ELECTRON CAPTURE

We shall concentrate on collision systems where the projectile charge Z_P is sufficiently larger than the target charge Z_T such that in a molecular description, the lowest electronic levels are well separated, in order to avoid strong coupling. We also want to restrict ourselves to the capture of a single target electron, and neglect the presence of the spectator electrons. The standard formula for the transition amplitude is given by

$$a_{fi} = \langle \psi_f^P(\infty) \mid U \psi_i^{(+)}(\infty) \rangle$$

$$-i \int_{-\infty}^{\infty} dt \left\langle \psi_f^P(t) \left| U \left[H - i \frac{\partial}{\partial t} \right] \right| \psi_i^{(+)}(t) \right\rangle , \quad (2.1)$$

where the electronic functions $\psi_i^{(+)}$ and ψ_f^P describe asymptotically an electron bound to the target (at $t \rightarrow -\infty$) and to the projectile (at $t \rightarrow +\infty$), respectively. As long as the wave functions are exact scattering solutions to the three-particle problem formula (2.1) is exact. If, on the other hand, trial functions are inserted into (2.1), a_{fi} is stationary with respect to variations of the

       © 1985 The American Physical Society

wave functions[11] and can thus be used as a starting point for variational calculations.

The electronic Hamiltonian H consists of the kinetic energy T, the projectile and target Coulomb fields, and the radiation field H_R. In the nonadiabatic sliding model, it is split into an unperturbed part H_0 from which the bound electronic states are derived, and a perturbation V by means of a parameter λ which later will be determined variationally. As rearrangement collisions are considered, the decomposition of H is taken to be different in the entrance and exit channel:

$$H = H_{0i} + H_R + V_f ,$$

$$H_{0i} = T - \frac{Z_T}{|\mathbf{r} - \mathbf{x}_i|} - \frac{\lambda Z_P}{|\mathbf{r} - \mathbf{R} - \mathbf{x}_i|} , \qquad (2.2a)$$

$$V_f = -(1-\lambda)\frac{Z_P}{|\mathbf{r} - \mathbf{R} - \mathbf{x}_i|} ;$$

$$H = H_{0f} + H_R + V_i ,$$

$$H_{0f} = T - \frac{Z_P}{|\mathbf{r}' - \mathbf{x}_f|} - \frac{\lambda Z_T}{|\mathbf{r}' + \mathbf{R} - \mathbf{x}_f|} , \qquad (2.2b)$$

$$V_i = -(1-\lambda)\frac{Z_T}{|\mathbf{r}' + \mathbf{R} - \mathbf{x}_f|} .$$

$\mathbf{R}(t)$ denotes the internuclear motion and the other coordinates are defined in Fig. 1. The initial state ψ_i^T is chosen as the eigenstate to H_{0i}, while the final state ψ_f^P is the eigenstate to H_{0f}. According to the choice of λ, they are preferentially atomic or molecular states.

The operator U in (2.1) describes the transformation from the "initial" rest frame of the electron (denoted by Σ) which is characterized by the location of $\psi_i^{(+)}$, i.e., centered a distance x_i off the target, to the "final" rest frame (Σ'), defined through the location of ψ_f^P, being a distance x_f away from the projectile (cf. Fig. 1). Note that both reference frames are sliding, because x_i and x_f are allowed to depend on time. The frame transformation, given by[14]
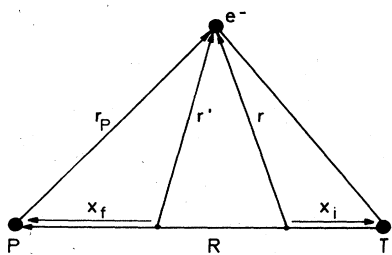

FIG. 1. Coordinates for the three-body system consisting of projectile (P), target (T), and electron (e). $\mathbf{r}$ and $\mathbf{r}'$ denote the location of the initial and final wave function, respectively, at a given internuclear separation R.

$$U = \exp\left[-i\int dt\tfrac{1}{2}(\dot{\mathbf{R}} + \dot{\mathbf{x}}_i - \dot{\mathbf{x}}_f)^2\right]$$

$$\times \exp[-i(\dot{\mathbf{R}} + \dot{\mathbf{x}}_i - \dot{\mathbf{x}}_f)\cdot\mathbf{r}']\exp[i(\mathbf{R} + \mathbf{x}_i - \mathbf{x}_f)\cdot\mathbf{p}] , \qquad (2.3)$$

where $\mathbf{p}$ is the conjugate momentum to $\mathbf{r}$, supplies the correct time-dependent translational factors.

When the Schrödinger operator is transformed to the system Σ', it becomes

$$U\left[H - i\frac{\partial}{\partial t}\right]U^\dagger = \begin{cases} E_f(t) + V_i(t) - i\dfrac{\partial}{\partial t} & (2.4a) \\[2ex] \dfrac{i}{c}e^{i\omega t}\mathbf{A}_\nu\cdot\left[\nabla_{\mathbf{r}'} - i\left(\dot{\mathbf{x}}_f - \dfrac{M_T}{M}\dot{\mathbf{R}}\right)\right] \end{cases} , \qquad (2.4b)$$

$$\mathbf{A}_\nu = \frac{c}{2\pi\sqrt{\omega}}\mathbf{u}_\nu ,$$

where the first expression (2.4a) is the transition operator for Coulomb capture, while (2.4b) is the transition operator for radiative capture in the dipole approximation. The equation $H_{0f}\psi_f^P = E_f\psi_f^P$ has been used, $\mathbf{u}_\nu$ is the polarization direction of the photon with frequency ω, and M_T is the target mass and M the total mass of projectile and target nuclei. Recoil effects (i.e., acceleration terms) have been neglected, which is a reasonable approximation if the restriction to small-angle scattering is made.

For the scattering state $\psi_i^{(+)}$, an approximation has to be chosen which is of higher order in the perturbation V_f to allow for a correct description of charge transfer. To this aim, we adopt a formulation in analogy to the strong-potential Born theory[15,16]

$$\psi_i^{(+)}(t) \approx \psi_i^T(t) + \int dt' G_f(t,t')V_f(t')\psi_i^T(t') , \qquad (2.5)$$

where the Green's function is given by $G_f(t,t') = [i\partial/\partial t - T - V_f(t) + i\epsilon]^{-1}\delta(t - t')$. It should be noted, however, that (2.5) agrees only in the case of $\lambda = 0$ with the strict definition of the strong-potential Born theory as a first-order expansion in the (weak) target field, while the projectile field is kept to all orders. In the molecular limit ($\lambda = 1$), on the other hand, where charge transfer has to be treated on the same footing as direct excitation, for which a first-order theory is sufficient, $V_f = 0$ and (2.5) leads indeed to the first Born approximation. Thus (2.5) provides the correct limiting cases, and moreover a smooth transition from a first-order to a higher-order theory as λ decreases.

For the transformation of $\psi_i^{(+)}$ to the system Σ', it is convenient to transform first to the projectile rest frame Σ_1 because in this system, the (reduced) projectile field V_f becomes time independent, such that the right-hand side of (2.5) can be easily evaluated. If a complete set of plane waves $|\mathbf{q}(\mathbf{r}_p)\rangle$ is introduced and the techniques of Ref. 17 applied, one obtains after a subsequent frame transformation $\Sigma_1 \rightarrow \Sigma'$

$$U\psi_i^{(+)} = \frac{1}{2\pi} \int dt' \int d\omega_0 \int d\mathbf{q}\, e^{-i\omega_0(t-t')} e^{-iE(\mathbf{q},t')} \varphi_i^T(\mathbf{q}+\mathbf{R}+\dot{\mathbf{x}}_i)$$

$$\times \exp\left[-i\int dt\,\dot{x}_f^2/2\right] e^{i\dot{\mathbf{x}}_f \cdot \mathbf{r}'}\left[1+\frac{1}{\omega_0-T-V_f+i\epsilon}V_f\right]|\mathbf{q}\rangle\,,$$

$$\tag{2.6}$$

$$E(\mathbf{q},t) = \tfrac{1}{2}\int dt(\dot{\mathbf{R}}+\dot{\mathbf{x}}_i)^2 + \int dt\,E_i - (\mathbf{q}+\dot{\mathbf{R}}+\dot{\mathbf{x}}_i)\cdot(\mathbf{R}+\mathbf{x}_i)\,,$$

where E_i is the energy of the initial state and φ_i^T its Fourier transform. The last bracket applied on $|\mathbf{q}\rangle$ defines an off-shell wave function $\psi_{\mathbf{q},\omega_0}$ with energy ω_0. In the following, we shall neglect off-shell effects and replace $\psi_{\mathbf{q},\omega_0}$ by a Coulomb wave $\psi_{\mathbf{q}}$. This impulse approximation gives results which for Coulomb capture are accurate within a factor of 2 for high collision velocities and are much better for radiative capture.[5] For slower collisions, on the other hand, the effect of both potentials is already built into the initial- and final-state wave functions, such that the omission of the extra potential dependence in the (intermediate) off-shell function should not play an important role. Then, (2.6) reduces to a single $\mathbf{q}$ integral, such that the transition amplitude (2.1) in the case of REC becomes

$$a_{fi} = \langle \psi_f^P(\infty)\,|\,U\psi_i^{(+)}(\infty)\rangle$$

$$-i\int_{-\infty}^{\infty} dt \int d\mathbf{q}\left\langle \psi_f^P(\mathbf{r}')\,\left|\frac{i}{c}e^{i\omega t}\mathbf{A}_\nu\cdot\left[\mathbf{\nabla}_{\mathbf{r}'}-i\dot{\mathbf{x}}_f+i\frac{M_T}{M}\dot{\mathbf{R}}\right]e^{i\dot{\mathbf{x}}_f\cdot\mathbf{r}'}\right|\psi_{\mathbf{q}}(\mathbf{r}'-\mathbf{x}_f)\right\rangle$$

$$\times\varphi_i^T(\mathbf{q}+\dot{\mathbf{R}}+\dot{\mathbf{x}}_i)e^{i\mathbf{q}\cdot(\mathbf{R}+\mathbf{x}_i)}\exp\left[i\int dt\{(E_f-E_i)-\tfrac{1}{2}[\dot{x}_f^2+(\dot{\mathbf{R}}+\dot{\mathbf{x}}_i)^2]\}+i(\dot{\mathbf{R}}+\dot{\mathbf{x}}_i)\cdot(\mathbf{R}+\mathbf{x}_i)\right]\,. \tag{2.7}$$

The first term in (2.7) vanishes because at $t\to\infty$, the phase $\exp[-iE(\mathbf{q},t)]$ of $U\psi_i^{(+)}(t)$ oscillates very rapidly. In the limiting case of $\lambda=1$ where $U\psi_i^{(+)}$ is just the transformed initial state, this term vanishes because at $t\to\infty$, the bound states ψ_i^T and ψ_f^P are localized an infinite distance apart. Thus the transition probability follows from the second term alone.

III. EVALUATION OF THE REC CROSS SECTION

An exact evaluation of the transition amplitude is rather complicated, because the wave functions which appear in (2.7) are localized at three different origins. As we are primarily interested in a qualitative description of the MO influence in the photon spectra, we shall resort to a simplified model problem where, however, the important physical aspects are retained.

Let us restrict ourselves to capture from the target K shell into the projectile K shell, a process which gives the dominant contribution to the tails of the REC spectrum. Then the two-center wave functions ψ_f^P and ψ_i^T correlate asymptotically to the projectile and target $1s$ states, respectively. If $Z_T < Z_P < 2Z_T$, which we shall assume in the following, ψ_i^T tends to the $2p$ state in the limit of united atoms. Otherwise, higher p states will be involved, which makes the calculation more cumbersome.

In order to avoid the handling of two-center functions, we approximate ψ_i^T and ψ_f^P also by means of a variational calculation. The ground-state $(1s\sigma)$ wave function ψ_f^P is, in the same way as for direct excitation,[13] obtained from the minimization of the expectation value of H_{0f}, calculated with a $1s$-like trial function $\psi_f^P = Z_f^{3/2}\pi^{-1/2}\exp(-Z_f r')$, with respect to the effective

charge Z_f and the location x_f.

The initial state ψ_i^T is also approximated by a one-center function. In order to allow for its $2p\sigma$ character, a linear combination between a $1s$ and $2p,m=0$ molecular hybrid state and an atomic $1s$ state is chosen

$$\psi_i^T(\mathbf{r}) = \frac{Z_i^{3/2}}{\sqrt{\pi}}\lambda\left[\gamma_1 e^{-Z_i r} + \frac{1}{4\sqrt{2}}\mu_1 e^{-Z_i r/2}Z_i\mathbf{r}\cdot\hat{\mathbf{R}}\right]$$

$$+\frac{Z_i^{3/2}}{\sqrt{\pi}}(1-\lambda)e^{-Z_i r}\,. \tag{3.1a}$$

The coefficients γ_1 and μ_1 of the hybrid state are determined from the normalization condition $\langle\psi_i^T\,|\,\psi_i^T\rangle=1$ together with the requirement that, for $\lambda=1$, ψ_i^T has to be orthogonal to the ground state,

$$\langle e^{-Z_f r'}\,|\,\gamma_1 e^{-Z_i r}+(1/4\sqrt{2})\mu_1 e^{-Z_i r/2}Z_i\mathbf{r}\cdot\hat{\mathbf{R}}\rangle=0\,. \tag{3.1b}$$

In accordance with the usual definition of the MO states, the quantization axis has been chosen along the internuclear coordinate $\mathbf{R}$. The state ψ_i^T is defined such that when λ varies from 1 to 0, ψ_i^T changes from a molecular state to an atomic one, while the condition of orthogonality to the ground state is more and more relaxed. There are two free parameters contained in this function, the charge Z_i as well as the location x_i.

In order to avoid an extended variational calculation, we have taken a predetermined value for x_i in our model. For very small λ, such that $\lambda Z_P \ll Z_T$ and ψ_i^T is approximately a target $1s$ state, x_i can be determined as in the case of the ground state through minimizing the expectation value of H_{0i}. In this limiting case, x_i is well described[18] by an analytical function of the internuclear distance

$$\frac{1}{R}x_i \equiv h_i = \frac{\lambda Z_P}{\lambda Z_P + Z_T}c_\lambda \frac{6}{y^3}[1-e^{-y}(\tfrac{1}{2}y^2+y+1)] \,,$$

$$y = 2Z_T R\left[\frac{Z_T}{\lambda Z_P+Z_T}\right]^{1/3}, \tag{3.2}$$

where y is proportional to R and determined from the correct asymptotic behavior $h_i \rightarrow 3\lambda Z_P/(4Z_T^4 R^3)$ for $R \rightarrow \infty$. Our approximation consists in applying formula

(3.2) for any value of λ. We have only changed the constant c_λ from its original value 1 to $c_\lambda = \lambda + (1-\lambda)Z_T/Z_P$ in order to account for a linear dependence of x_i on λ for small λ even when $\lambda Z_P > Z_T$, which induces a faster approach to the atomic case than $c_\lambda = 1$. For $Z_P = Z_T$ or $\lambda = 1$, c_λ is unchanged.

The effective charge Z_i is obtained from a variational calculation by minimizing the expectation value of H_{0i}, $\partial E_i/\partial Z_i = 0$, with

$$E_i \equiv \langle \psi_i^T \mid H_{0i} \mid \psi_i^T \rangle = \frac{Z_i^2}{8}(1+3\gamma_2^2) - Z_T[\gamma_2^2 M_0(h_i,Z_i) - \gamma_2\mu_2 M_1(h_i,Z_i) + \mu_2^2 M_2(h_i,Z_i)]$$

$$- \lambda Z_P[\gamma_2^2 M_0(1-h_i,Z_i) + \gamma_2\mu_2 M_1(1-h_i,Z_i) + \mu_2^2 M_2(1-h_i,Z_i)] \,,$$

$$M_0(h_i,Z_i) = Z_i\left[\frac{1}{\rho} - e^{-2\rho}\left(1+\frac{1}{\rho}\right)\right], \quad \rho = Z_i h_i R \tag{3.3}$$

$$M_1(h_i,Z_i) = \frac{4\sqrt{2}}{9}Z_i\left[\frac{64}{27\rho^2} - e^{-3\rho/2}\left(\rho + \frac{8}{3} + \frac{32}{9\rho} + \frac{64}{27\rho^2}\right)\right] \,,$$

$$M_2(h_i,Z_i) = Z_i\left[\frac{1}{\rho} + \frac{12}{\rho^3} - e^{-\rho}\left(\frac{\rho^2}{8} + \frac{3}{4}\rho + \frac{11}{4} + \frac{7}{\rho} + \frac{12}{\rho^2} + \frac{12}{\rho^3}\right)\right] \,,$$

where $x_i = -h_i R$ has been inserted, while γ_2 and μ_2 are the s-wave and p-wave coefficients of ψ_i^T, viz., $\mu_2 = \lambda\mu_1$, $\gamma_2 = \lambda\gamma_1 + 1 - \lambda$, which also depend on Z_i. The resulting effective charge has the correct limiting values, as it tends to $Z_T + \lambda Z_P$ for $R \rightarrow 0$, and to Z_T for $R \rightarrow \infty$. Correspondingly, the energy E_i of the initial state is $-[1+3(1-\lambda)^2](Z_T+\lambda Z_P)^2/8$ for $R=0$ and $-Z_T^2/2$ for $R \rightarrow \infty$. For $R=0$, the energy thus varies from $-(Z_P+Z_T)^2/8$ for $\lambda=1$ to $-Z_T^2/2$ for $\lambda=0$. Figure 2 shows $E_i(R)$ and $E_f(R)$ for the system $^{16}O \rightarrow {}^{12}C$ for various choices of λ. For the molecular case $\lambda=1$, we have also estimated the $1s\sigma$ and $2p\sigma$ energies from a linear combination of atomic orbitals calculation including the $1s$ and $2p,m=0$ projectile states and the $1s$ target state. A comparison reveals that the R dependence is rather similar in both calculations, but that the united-atom limiting values are only correctly reproduced by the variational calculation.

The intermediate continuum state $\psi_q(r'-x_f)$ which also enters into (2.7), is an eigenfunction to a Coulomb field with effective charge $(1-\lambda)Z_P$, localized on the projectile. It is the product of a hypergeometric function $_1F_1$ and a phase $\exp[iq\cdot(r'-x_f)]$. In order to avoid a three-center calculation, we retain the correct origin only in the phase, but neglect the shift x_f between Σ_1 and Σ' in the remainder of ψ_q. This has no influence on the translational factors, and also preserves the correct limiting cases $\lambda=0$ and $\lambda=1$ (for $\lambda=0$, $x_f=0$, while for $\lambda=1$, $_1F_1=1$).

For the evaluation of the transition matrix element we define the basic integral

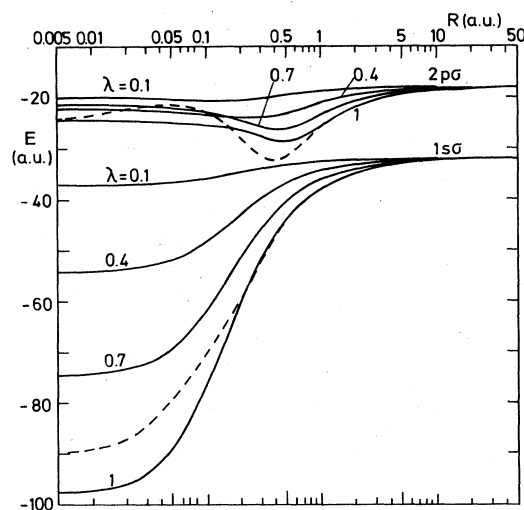FIG. 2. Correlation diagram for the $1s\sigma$ and $2p\sigma$ states of the system $^{16}O + {}^{12}C$ as a function of the internuclear separation R, with different choices of λ (solid curves). Also shown is the result of a three-state close-coupling calculation (dashed curves) which should be compared with the sliding result for $\lambda=1$.

$$F_q(Z_f, \dot{\mathbf{x}}_f) = \text{const} \left\langle \psi_f^P(\mathbf{r}') \left| \frac{1}{r'} e^{i\dot{\mathbf{x}}_f \cdot \mathbf{r}'} \right| \psi_\mathbf{q}(\mathbf{r}') \right\rangle$$

$$= \int d\mathbf{r}' \frac{e^{-Z_f r'}}{r'} e^{i\dot{\mathbf{x}}_f \cdot \mathbf{r}'} e^{i\mathbf{q}\cdot\mathbf{r}'} \, {}_1F_1(i\eta, 1, i(qr' - \mathbf{q}\cdot\mathbf{r}'))$$

$$= \frac{4\pi}{Z_f^2 + (\dot{\mathbf{x}}_f + \mathbf{q})^2} \left[\frac{\dot{x}_f^2 - (q + iZ_f)^2}{Z_f^2 + (\dot{\mathbf{x}}_f + \mathbf{q})^2} \right]^{-i\eta}, \quad \eta = (1-\lambda)Z_P/q \ . \tag{3.4}$$

Then, with $-i\nabla_r \exp(-Z_f r) = iZ_f \hat{\mathbf{r}} \exp(-Z_f r)$, the transition operator can be written by means of partial derivatives of F_q, such that the transition amplitude becomes, with the definition $\mathbf{R} + \mathbf{x}_i = -\mathbf{q}_0$,

$$a_{fi} = -i \int dt \, \mathbf{I}_q(t) \cdot \frac{i}{c} \mathbf{A}_\nu e^{i\omega t} \exp\left[i \int dt [(E_f - E_i) - \tfrac{1}{2}(\dot{x}_f^2 + q_0^2)] \right] \exp[-i\mathbf{q}_0 \cdot (\mathbf{R} + \mathbf{x}_i)] \ ,$$

$$\mathbf{I}_q(t) = \frac{1}{\sqrt{\pi}} Z_f^{3/2} \int d\mathbf{q} \, e^{-i\mathbf{q}\cdot\mathbf{x}_f} N_q e^{i\mathbf{q}\cdot(\mathbf{R}+\mathbf{x}_i)} \varphi_i^T(\mathbf{q}-\mathbf{q}_0) \left[-iZ_f \frac{d}{d\dot{\mathbf{x}}_f} + i \left[\dot{\mathbf{x}}_f - \frac{M_T}{M} \dot{\mathbf{R}} \right] \frac{d}{dZ_f} \right] F_q(Z_f, \dot{\mathbf{x}}_f) \ , \tag{3.5}$$

$$N_q = (2\pi)^{-3/2} e^{\pi\eta/2} \Gamma(1 - i\eta) \ .$$

From the function (3.1a), the Fourier transform φ_i^T is easily calculated:

$$\varphi_i^T(\mathbf{p}) = -\gamma_2 \frac{\sqrt{2}}{\pi} Z_i^{3/2} \frac{d}{dZ_i} \left[\frac{1}{Z_i^2 + p^2} \right]$$

$$-i\mu_2 \frac{Z_i^{5/2}}{2\pi} \hat{\mathbf{R}} \cdot \frac{d}{d\mathbf{p}} \frac{d}{dZ_i} \left[\frac{1}{p^2 + Z_i^2/4} \right] \ . \tag{3.6}$$

For the evaluation of the integral over the momentum transfer $\mathbf{q}$ in (3.5) which is complicated through the presence of $N_q F_q$, we introduce a peaking approximation. Making use of the fact that the presence of the Fourier transform $\varphi_i^T(\mathbf{q}-\mathbf{q}_0)$ selects momentum values strongly localized around $\mathbf{q}_0$, we replace $\mathbf{q}$ in the η-dependent part of F_q and in N_q by $\mathbf{q}_0$. This peaking approximation is irrelevant in the case of $\lambda \to 1$ because then $\eta = 0$, but it is most restrictive in the other limiting case, $\lambda \to 0$ $(\eta \to Z_P/q)$. However, it is known that for fast collisions, the peaked impulse approximation is a very good approximation for capture to the K shell of a heavy projectile.[2,3]

From the transition amplitude, the differential cross section for photon emission into the solid angle $d\Omega$ is obtained through an integration over impact parameter b and a summation over the polarization direction ν,

$$\frac{d^2\sigma}{d\omega \, d\Omega} = 2 \sum_{\nu=1,2} \frac{2\pi\omega^2}{c^3} \int_0^\infty b \, db \, |a_{fi}|^2 \ , \tag{3.7}$$

where a factor of 2 has been included because of the two K electrons to be captured. The dependence of a_{fi} on b enters through the choice of the internuclear trajectory $\mathbf{R}(t)$ which is taken as a Rutherford hyperbola. Details of the evaluation of (3.7) are given in the Appendix.

Before formula (3.7) or its explicit form (A6) can be used to extract results, the auxiliary parameter λ has to be determined, i.e., the "best" wave functions have to be

found. According to Demkov's theory, this can be done by requiring that the transition probability be stationary with respect to variations in λ. This leads to a (real) "adiabaticity" parameter λ which depends on the collision velocity but not explicitly on time such that the global nonadiabaticity can be extracted. However, from the requirement that $|a_{fi}|^2$ be an extremum, λ will depend on impact parameter, and this dependence is much stronger than in the case of direct excitation. As the present REC experiments do not differentiate with respect to b, it seems more appropriate to choose a λ which takes the whole collision dynamics globally into account. Thus we determine λ from the prescription

$$\frac{d}{d\lambda} \left[\frac{d^2\sigma}{d\omega \, d\Omega} \right] = 0 \ . \tag{3.8}$$

While in the case of direct excitation and Coulomb capture the optimized value of λ is determined from the balance of a potential part and the time derivative in the transition operator, things are different for radiative capture. Here, the balance has to be provided by the transition matrix element on one hand, and by the energy phase through its strong ω dependence on the other hand. In the REC peak region, the cross section is large, because the energy phase is small at approximately zero momentum transfer[5] $(\mathbf{q} \approx -\mathbf{v})$. This requires $\lambda \to 0$ because, otherwise, $(\mathbf{R} + \dot{\mathbf{x}}_i - \dot{\mathbf{x}}_f)^2/2 \ll v^2/2$, making the energy phase large and damping the integral. However, for frequencies well above or below the peak, a large momentum transfer to the electron is required. In that case, a high value of λ is favorable, as molecular functions with a bigger effective charge can provide higher-momentum components, enhancing the transition matrix element. From this argumentation it follows immediately that the cross section has a *maximum* at the optimized value of λ.

IV. NUMERICAL RESULTS

We have performed calculations for the two collision systems $^{16}O \rightarrow ^{12}C$ and $^{32}S \rightarrow ^{20}Ne$ at two different velocities. We have only considered the purely hydrogenic case and neglected all screening effects.

The results for the parameter λ as a function of photon energy are shown in Fig. 3. Around the value of the REC peak $(\omega_{peak} = v^2/2 + E_i - E_f)$, the maximum determined by (3.8) is found at $\lambda = 0$. When ω increases, λ begins to rise rather suddenly, indicating the importance of molecular effects. At some value of ω, however, the maximum of the differential cross section flattens out and eventually disappears. Then λ can no longer be determined from (3.8). This happens around $\lambda \simeq 0.5$.

In order to elucidate these rather unexpected findings, our simplified model has to be reexamined. Let us recall that two important assumptions enter into that model, the prescription of the location $x_i(R)$ of the initial state, and the choice of the p admixture in ψ_i^T. In order to test the stability of the model, we have changed these assumptions. For example, we have dropped the prefactor c_λ in the definition (3.2) of x_i, and in another run have taken x_i to be proportional to x_f with a proportionality constant Z_P/Z_T. On the other hand, we have defined the p admixture with a space-fixed quantization axis along $\mathbf{v}$. This would account for the predictions that due to the coupling between the $2p, m = 0$ and the $2p, m = \pm 1$ states in slow collisions, the effective quantization axis remains fixed in space.[9] When λ is calculated from these different prescriptions, no qualitative change in its behavior is observed, however. In particular, the steep rise of λ in a narrow range of ω, as well as the disappearance of the maximum in the differential cross section at some high value of ω is still present. This gives some confidence in that the results from Fig. 3 are not just accidental.

Also, on the low-energy side of ω_{peak}, there is a rise of λ with increasing difference $\omega_{peak} - \omega$. As for the high-energy side, this behavior arises from an enhanced momentum transfer to the electron as soon as the energy phase $F(t)$ deviates from zero: In order to avoid a rapidly
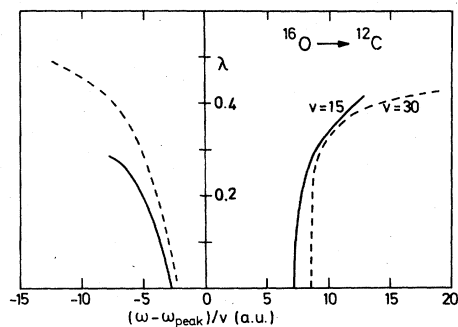
oscillating phase, the relative velocity together with the energies E_i and E_f have to be chosen to be strongly time dependent. Together with a matrix element which provides enhanced high-momentum components through an increased central charge, it follows that a molecular influence leads to a higher cross section. On the other hand, if the molecular admixture (i.e., λ) is chosen too large, the energy phase will for $\omega \gg \omega_{peak}$ increase again because the contribution from the relative velocity gradually diminishes, implying a reduction of the cross section. This competition might explain the steep rise from the atomic description to a molecularlike description on the high-energy side. On the low-energy side, the phase will decrease when the relative velocity decreases. Thus the onset of the molecular influence occurs at frequencies which are much closer to ω_{peak} than on the high-energy side, and λ is much higher for the same $|\omega - \omega_{peak}|$.

In the atomic picture, the phase is given by $F(t) = (\omega - \omega_{peak})t \approx (\omega - \omega_{peak})R/v$ for a straight-line trajectory. From this one expects an approximate scaling behavior of the cross section with $(\omega - \omega_{peak})/v$ if the influence of the phase dominates the matrix element. This is indeed verified in Fig. 3 where the calculation is performed for a velocity which is roughly equal to the united-atom K-shell velocity $Z_P + Z_T$, and for a velocity twice as large. When the scaling is used, the difference in λ for these two velocities is not very large. For the system $^{16}O + ^{12}C$, which is more symmetric $(Z_P/Z_T = 1.3)$ than the system $^{32}S + ^{20}Ne$ $(Z_P/Z_T = 1.6)$, the molecular behavior is more pronounced, which shows itself in an earlier onset of the increase of λ in units of the scaled frequency.

As a given phase selects a certain value of momentum transfer and thus the corresponding Fourier component of the electronic wave function, the approximate scaling should also hold for the shape of the REC peak. This is displayed in Fig. 4 where the differential cross section for K-K capture is shown for the system $^{16}O \rightarrow ^{12}C$ as a func-
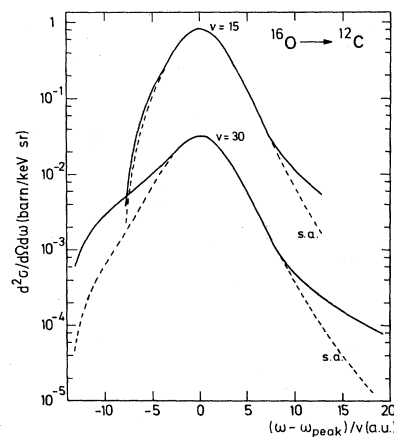

FIG. 3. λ as a function of the scaled photon frequency $(\omega - \omega_{peak})/v$ for K-K transfer in $^{16}O + ^{12}C$ collisions. Photon emission angle is $\vartheta = 90°$. Solid curves are calculated for a collision velocity of 15 a.u., dashed curves for $v = 30$ a.u.

FIG. 4. Doubly differential cross section for photon emission at $\vartheta = 90°$ in the system $^{16}O + ^{12}C$ as a function of the scaled photon frequency. Calculations are performed for the collision velocities $v = 15$ and 30 a.u. Solid curves are the results from the sliding-center model, dashed curves are calculated with the impulse approximation (i.e., $\lambda = 0$; separated atom).
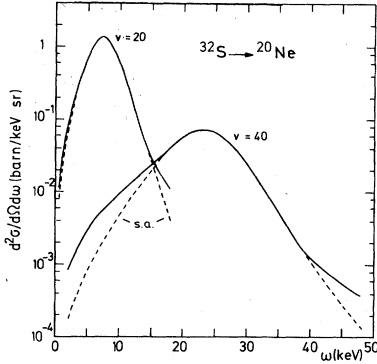
FIG. 5. Doubly differential cross section for photon emission at $\vartheta = 90°$ in the system $^{32}S + ^{20}Ne$ as a function of photon energy ω. Calculations are performed for the collision velocities $v = 20$ and 40 a.u. Solid curves are the results from the sliding-center model, dashed curves are calculated with the impulse approximation.

tion of the scaled frequency. At the high-energy side, the slope for the two chosen velocities is nearly identical, both for the atomic theory (where it is known that the peak width increases linearly[3] with v) and for the present sliding theory. This is no longer true for the low-energy wing, where the increasing importance of the matrix element makes the scaling (which is based on the behavior of the phase alone) invalid. It is evident both from Fig. 4 and from Fig. 5, which displays the results for the $^{32}S + ^{20}Ne$ collision system, that the REC cross section attains much larger values in the tails of the spectrum when the calculations are performed within the sliding model instead of within a purely atomic theory.

V. CONCLUSION

We have formulated a theory for electron capture which includes the freedom of choice between atomic and molecular basis states. An optimization procedure is introduced where it is required that the transition probability becomes stationary with respect to variations of the wave functions. For Coulomb capture, where this requirement is achieved by means of the balance between the two parts of the transition operator, the Coulomb field and the time derivative, a high collision velocity requires an atomic description, while the molecular influence becomes gradually larger when v decreases. For radiative capture, on the other hand, it is the transition matrix element of the radiation field and the frequency-dependent energy phase which have to be equilibrated. When the photon distribution is considered, the molecular effects increase only marginally when the velocity is lowered. Rather, for the high-frequency wing (beyond the REC peak) the intensity scales with $(\omega - \omega_{peak})/v$. Around the REC peak, an atomic description has to be used, while on both wings the molecular effects become increasingly important the larger $|\omega - \omega_{peak}|$, even for very fast collisions. These molecular effects give rise to an enhancement of the cross section in accordance with the experimental findings.

A quantitative comparison with experiment is not yet possible at this stage. To this aim, transitions from higher target shells, which provide the dominant contribution to the peak region, have to be included. Further, the lack of a stationary point in our model for the cross section at frequencies exceeding a certain high value excludes a comparison with the complete experimental tail region.

These difficulties might be overcome by choosing a more realistic approximation for the initial state, i.e., a two-center function, and perhaps also by allowing for a superposition of the degenerate p states with different m quantum numbers. However, this would involve a great numerical effort and lies outside the scope of the present paper.

ACKNOWLEDGMENTS

APPENDIX

In this appendix the differential cross section for photon emission is explicitly evaluated.

After the application of the peaking approximation, the integrand $I_q(t)$ of the transition amplitude (3.5) can be written in the following way [with $\eta_0 = (1 - \lambda)Z_P/q_0$]:

$$I_q(t) = 4\sqrt{\pi}Z_f^{3/2}N_{q_0}\left[-iZ_f\frac{d}{d\dot{x}_f} + \left[i\dot{x}_f - i\frac{M_T}{M}\dot{R}\right]\frac{d}{dZ_f}\right]\left[\left[\frac{\dot{x}_f^2 - (q_0 + iZ_f)^2}{Z_f^2 + (\dot{x}_f + q_0)^2}\right]^{-i\eta_0}S(Z_f,\dot{x}_f)\right],$$

(A1)

$$S(Z_f,\dot{x}_f) = \int d\mathbf{q}\, e^{-i\mathbf{q}\cdot(\mathbf{x}_f - \mathbf{R} - \mathbf{x}_i)}\varphi_i^T(\mathbf{q} - \mathbf{q}_0)\frac{1}{Z_f^2 + (\dot{x}_f + \mathbf{q})^2}$$

$$= e^{-i\mathbf{q}_0\cdot(\mathbf{x}_f - \mathbf{R} - \mathbf{x}_i)}\left[-\gamma_2\frac{\sqrt{2}}{\pi}Z_i^{3/2}\frac{d}{dZ_i}J(Z_i,\dot{x}_f + \mathbf{q}_0)\right.$$

$$\left. - i\mu_2\frac{Z_i^{5/2}}{2\pi}\hat{\mathbf{R}}\cdot\frac{d}{dZ_i}\frac{d}{d\mathbf{s}}[e^{i\mathbf{s}\cdot(\mathbf{x}_f - \mathbf{R} - \mathbf{x}_i)}J(Z_i/2,\dot{x}_f + \mathbf{q}_0 - \mathbf{s})]_{s=0}\right],$$

where the transformation $\mathbf{p} = \mathbf{q} - \mathbf{q}_0$ has been introduced, and the explicit form of $\varphi_i^T(\mathbf{p})$, (3.6), has been inserted. The auxiliary function $J(Z, \mathbf{d})$ is defined by

$$J(Z, \mathbf{d}) = \int d\mathbf{p}\, e^{-i\mathbf{p} \cdot \mathbf{b}_{fi}} \frac{1}{Z_f^2 + (\mathbf{p} + \mathbf{d})^2} \frac{1}{Z^2 + p^2} \,,$$

$$\mathbf{b}_{fi} = \mathbf{x}_f - \mathbf{R} - \mathbf{x}_i \,. \quad \text{(A2)}$$

It can be reduced to a single (numerically fast-converging) integral with the double-integral representation of an inverse product

$$\frac{1}{ac} = \int_0^1 dy\, \frac{1}{[ay + c(1-y)]^2}$$

$$= \int_0^1 dy \int_0^\infty d\xi\, \xi e^{-[ay + c(1-y)]\xi} \,. \quad \text{(A3)}$$

Then, the $\mathbf{p}$ integration can easily be done by means of quadratic completion in the exponent plus a linear variable shift. Also, the integration over ξ can be evaluated, such that

$$J(Z, \mathbf{d}) = \pi^{3/2} \int_0^1 dy\, e^{i\mathbf{b}_{fi} \cdot \mathbf{d}y} \int_0^\infty d\xi\, \xi^{-1/2} e^{-b_{fi}^2/4\xi} e^{-\alpha\xi}$$

$$= \pi^2 \int_0^1 dy\, e^{i\mathbf{b}_{fi} \cdot \mathbf{d}y} \frac{1}{\sqrt{\alpha}} e^{-b_{fi}\sqrt{\alpha}} \,,$$

$$\alpha = Z_f^2 y + d^2 y(1-y) + Z^2(1-y) > 0 \,. \quad \text{(A4)}$$

For the calculation of the remaining time integral, we choose a coordinate system where the variables have symmetry properties under time reversal. The x axis is taken along the internuclear coordinate at the distance of closest approach, and the z axis perpendicular to it in the collision plane, such that the angle between the collision velocity $\mathbf{v}$ and the z axis is equal to $\theta/2$, where θ is the scattering angle. In this coordinate system, the quantities R, R_x, $\dot{R}_z$, x_f, and x_i are even if t is replaced by $-t$, while R_z, $\dot{R}_x$, $\dot{x}_f$, and $\dot{x}_i$ change sign. With these properties, the time integration interval can be reduced to $(0, \infty)$.

If the photon is ejected with an angle ϑ with respect to the beam direction $\hat{\mathbf{v}}$, the two possible polarization directions $\mathbf{u}_\nu$ can be chosen as[5]

$$\mathbf{u}_1 = (0, 1, 0) \,,$$

$$\mathbf{u}_2 \equiv (u_x, 0, u_z) = (-\cos\vartheta \cos(\theta/2) - \sin\vartheta \sin(\theta/2), 0, \sin\vartheta \cos(\theta/2) - \cos\vartheta \sin(\theta/2)) \quad \text{(A5)}$$

As the only direction which appears in the integrand $\mathbf{I}_q(t)$ arises from the combination of $\mathbf{R}$ and its derivative, which both lie in the (x, z) plane, $\mathbf{u}_1$ does not give any contribution to the transition amplitude.

Collecting all results, the final formula is obtained:

$$\frac{d^2\sigma}{d\omega\, d\Omega} = \frac{8\omega}{\pi c^3} \int_0^\infty b\, db \left| \int_0^\infty dt\, Z_f^{3/2} Z_i^{5/2} e^{\pi\eta_0/2} \Gamma(1 - i\eta_0) \left[\frac{\dot{x}_f^2 - (q_0 + iZ_f)^2}{Z_f^2 + (\dot{x}_f + q_0)^2} \right]^{-i\eta_0} \right.$$

$$\times \int_0^1 dy(1-y)\{ \cos[F(t) + \mathbf{b}_{fi} \cdot \mathbf{d}y](G_1 G_2 + W_1 W_2 + C_0 G_5 + C_1 G_6)$$

$$\left. + i\, \sin[F(t) + \mathbf{b}_{fi} \cdot \mathbf{d}y](G_1 W_2 + W_1 G_2 + C_0 W_5 + C_1 W_6)\} \right|^2 \,,$$

$$\quad \text{(A6)}$$

$$F(t) \equiv \omega t + \int dt(E_f - E_i) - \tfrac{1}{2} \int dt(\dot{\mathbf{R}} + \dot{\mathbf{x}}_i - \dot{\mathbf{x}}_f)^2 \,.$$

For the numerical evaluation of the time integral, it is convenient to use a pseudolinear coordinate[13] τ, which is obtained from the usual hyperbolic coordinate w through the transformation $\tau = \epsilon \exp(w)$ where $\epsilon = [\sin(\theta/2)]^{-1}$.

In (A6), the following definitions have been introduced, with $\mathbf{d} \equiv (d_x, 0, d_z) = \mathbf{x}_f + \mathbf{q}_0$, $\mathbf{x}_f = (\dot{x}_x, 0, \dot{x}_z)$, and $\mathbf{b}_{fi} = (b_x, 0, b_z)$:

$$\begin{bmatrix} G_1 \\ W_1 \end{bmatrix} = 2\eta_0 \begin{bmatrix} u_z \\ u_x \end{bmatrix} \left\{ \frac{1}{\dot{x}_f^2 - (q_0 + iZ_f)^2} \left[-iq_0 \begin{bmatrix} \dot{x}_z \\ \dot{x}_x \end{bmatrix} + \frac{M_T}{M} \begin{bmatrix} \dot{R}_z \\ \dot{R}_x \end{bmatrix} \right] (iq_0 - Z_f) + \frac{Z_f}{Z_f^2 + (\dot{x}_f + q_0)^2} \left[\begin{bmatrix} q_{0z} \\ q_{0x} \end{bmatrix} + \frac{M_T}{M} \begin{bmatrix} \dot{R}_z \\ \dot{R}_x \end{bmatrix} \right] \right\} \,,$$

$$G_2 = \gamma_2 \sqrt{2} e^{-b_{fi}(\alpha_0)^{1/2}} \left[\frac{1}{\alpha_0^{3/2}} + \frac{b_{fi}}{\alpha_0} \right] - (1-y)\mu_2 \frac{Z_i}{8R} e^{-b_{fi}(\alpha_1)^{1/2}} \mathbf{b}_{fi} \cdot \mathbf{R} \left[\frac{b_{fi}}{\alpha_1} + \frac{1}{\alpha_1^{3/2}} \right] \,,$$

$$W_2 = (1-y)\mu_2 \frac{Z_i}{4R} e^{-b_{fi}(\alpha_1)^{1/2}} iy\mathbf{d} \cdot \mathbf{R}\beta_1 \,,$$

$$\begin{bmatrix} G_5 \\ W_5 \end{bmatrix} = -i \begin{bmatrix} b_x u_x \\ b_z u_z \end{bmatrix} \left[\frac{1}{\alpha_0^{3/2}} + \frac{b_{fi}}{\alpha_0} \right] + \begin{bmatrix} u_z \\ u_x \end{bmatrix} \left[\begin{bmatrix} d_z \\ d_x \end{bmatrix} (1-y) - \begin{bmatrix} \dot{x}_z \\ \dot{x}_x \end{bmatrix} + \frac{M_T}{M} \begin{bmatrix} \dot{R}_z \\ \dot{R}_x \end{bmatrix} \right] \left[\frac{3}{\alpha_0^{5/2}} + \frac{3 b_{fi}}{\alpha_0^2} + \frac{b_{fi}^2}{\alpha_0^{3/2}} \right] ,$$

$$\begin{bmatrix} G_6 \\ W_6 \end{bmatrix} = \frac{i}{2} \mathbf{b}_{fi} \cdot \mathbf{R} \begin{bmatrix} b_x u_x \\ b_z u_z \end{bmatrix} \left[\frac{b_{fi}}{\alpha_1} + \frac{1}{\alpha_1^{3/2}} \right] - \begin{bmatrix} u_z \\ u_x \end{bmatrix} \left[\begin{bmatrix} d_z \\ d_x \end{bmatrix} (1-y) - \begin{bmatrix} \dot{x}_z \\ \dot{x}_x \end{bmatrix} + \frac{M_T}{M} \begin{bmatrix} \dot{R}_z \\ \dot{R}_x \end{bmatrix} \right] \beta_1 \mathbf{b}_{fi} \cdot \mathbf{R}$$

$$- \begin{bmatrix} u_x \\ u_z \end{bmatrix} \left[\begin{bmatrix} d_x \\ d_z \end{bmatrix} (1-y) - \begin{bmatrix} \dot{x}_x \\ \dot{x}_z \end{bmatrix} + \frac{M_T}{M} \begin{bmatrix} \dot{R}_x \\ \dot{R}_z \end{bmatrix} \right] \beta_2 \mathbf{d} \cdot \mathbf{R} + \beta_1 \left[\begin{bmatrix} b_z u_z \\ b_x u_x \end{bmatrix} y \mathbf{d} \cdot \mathbf{R} - i \begin{bmatrix} R_x u_x \\ R_z u_z \end{bmatrix} \right] ,$$

$$C_0 = i Z_f y \gamma_2 \sqrt{2} e^{-b_{fi}(\alpha_0)^{1/2}} , \quad C_1 = i Z_f \mu_2 \frac{1}{4R} Z_i y (1-y) e^{-b_{fi}(\alpha_1)^{1/2}} ,$$

$$\alpha_0 = Z_f^2 y + d^2 y (1-y) + Z_i^2 (1-y) , \quad \alpha_1 = Z_f^2 y + d^2 y (1-y) + \frac{Z_i^2}{4} (1-y) ,$$

$$\beta_1 = \frac{1}{2} \left[\frac{b_{fi}^2}{\alpha_1^{3/2}} + \frac{3 b_{fi}}{\alpha_1^2} + \frac{3}{\alpha_1^{5/2}} \right] , \quad \beta_2 = -i y \left[\frac{3 b_{fi}^2}{\alpha_1^{5/2}} + \frac{b_{fi}^3}{2\alpha_1^2} + \frac{15 b_{fi}}{2\alpha_1^3} + \frac{15}{2\alpha_1^{7/2}} \right] .$$

(A7)

---

[1] K. W. Schnopper, H.-D. Betz, J. P. Delvaille, K. Kalata, A. R. Sohval, K. W. Jones, and H. E. Wegner, Phys. Rev. Lett. 29, 898 (1972).

[2] P. Kienle, M. Kleber, B. Povh, R. M. Diamond, F. S. Stephens, E. Grosse, M. R. Maier, and D. Proetel, Phys. Rev. Lett. 31, 1099 (1973).

[3] M. Kleber and D. H. Jakubassa, Nucl. Phys. A252, 152 (1975).

[4] E. Spindler, H.-D. Betz, and F. Bell, J. Phys. B 10, L561 (1977); E. Spindler, Ph.D. thesis, University of Munich, 1979.

[5] D. H. Jakubassa-Amundsen, R. Höppler, and H.-D. Betz, J. Phys. B 17, 3943 (1984).

[6] D. H. Jakubassa and M. Kleber, Z. Phys. A 273, 29 (1975).

[7] H.-D. Betz, F. Bell, H. Panke, W. Stehling, E. Spindler, and M. Kleber, Phys. Rev. Lett. 34, 1256 (1975).

[8] J. S. Briggs, J. H. Macek, and K. Taulbjerg, J. Phys. B 12, 1457 (1979).

[9] R. Anholt, Z. Phys. A 288, 257 (1978).

[10] P. M. Stevenson, Phys. Rev. D 23, 2916 (1981).

[11] Y. N. Demkov, Zh. Eksp. Teor. Fiz. 38, 1879 (1960) [Sov. Phys.—JETP 11, 1351 (1960)].

[12] D. H. Jakubassa, Z. Phys. A 290, 13 (1979).

[13] D. H. Jakubassa-Amundsen, Z. Phys. A 320, 557 (1985).

[14] P. A. Amundsen, J. Phys. B 11, 3197 (1978).

[15] J. Macek and S. Alston, Phys. Rev. A 26, 250 (1982).

[16] P. A. Amundsen and D. H. Jakubassa-Amundsen, J. Phys. B 17, 2671 (1984).

[17] D. H. Jakubassa-Amundsen and P. A. Amundsen, Z. Phys. A 297, 203 (1980).

[18] R. Anholt, Z. Phys. A 295, 201 (1980).